

# CONVENTIONAL DTI AND Q-SPACE IMAGING IN BRACHIAL PLEXUS ROOT RE-IMPLANTATION

Torben Schneider<sup>1</sup>, Xun Choong<sup>2</sup>, Carolina Kachramanoglou<sup>3</sup>, David L Thomas<sup>2</sup>, David Choi<sup>4</sup>, Claudia A M Wheeler-Kingshott<sup>1</sup>, and Olga Ciccarelli<sup>2</sup>

<sup>1</sup>NMR Research Unit, Queen Square MS Centre, Department of Neuroinflammation, UCL Institute of Neurology, London, United Kingdom, <sup>2</sup>Department of Brain Repair and Rehabilitation, UCL Institute of Neurology, London, United Kingdom, <sup>3</sup>Spinal Repair Unit, UCL Institute of Neurology, London, United Kingdom, <sup>4</sup>Department of Neurosurgery, National Hospital for Neurology and Neurosurgery, London, United Kingdom

## INTRODUCTION

Complete brachial plexus avulsion (BPA) is a devastating injury that occurs most commonly in young adults after motorcycle accidents and leads to a completely paralysed and anaesthetic limb. Re-implantation of avulsed ventral roots is an effective surgical technique that leads to improved motor recovery<sup>1</sup>. Structural MRI is insensitive to BPA, as the spinal cord in BPA appears normal. Diffusion weighted imaging (DWI) can provide better characterisation of BPA as it is sensitive to microscopic changes of tissue, including axonal damage or neuronal death, promising better non-invasive markers for therapy monitoring. Diffusion tensor imaging is a simple DWI analysis method, which is routinely used to study the microstructure of healthy and diseased nervous tissue. Q-space imaging<sup>2</sup> (QSI) is a technically more demanding DWI technique, which promises a more complete description of the diffusion probability density function (dPDF). We aimed to assess whether DTI or QSI of the upper cervical cord (i.e., above the site of injury) detects pathological changes in patients with BPA who have received re-implantation, when compared with healthy subjects. In patients, the relationship between QSI and DTI imaging markers and clinical outcome measures is explored.

## METHODS

**Study design:** We recruited 19 healthy subjects and 10 patients treated with re-implantation. In each patient the complete avulsion injury was confirmed by direct visualisation of the brachial plexus and re-implantation was performed within 1 month of injury. Patient disability was assessed using the following scales: (i) Disability for Arm, Shoulder and Hand (DASH) questionnaire, (ii) Visual Analogue Pain Scale (VAS) self assessment of pain (iii) Medical Research Council (MRC) muscle strength assessment of 7 muscle groups for the upper limb.

**MRI:** For each subject QSI and DTI datasets were acquired at cervical cord level using the posterior part of an 8-channel head coil, standard neck and upper-most spine coils. Imaging parameters were as follows: acquisition matrix=96x96, interpolated to 192x192, FOV=144x144mm<sup>2</sup>, slice thickness=5mm, 20 slices, TE=88ms/120ms (DTI/QSI), TR ≈ 4000ms (cardiac-gated). Four datasets (2 healthy/2 patients) were excluded because of incorrect acquisition or severe artifacts.

**QSI protocol:** The acquired QSI dataset contained 2 non-diffusion-weighted (b=0) and 30 DWI volumes with b-values between 50-3000s/mm<sup>2</sup> in b=50s/mm<sup>2</sup> steps (gradient duration=45ms, diffusion time=55ms, maximum gradient strength=23mT/m). Three different DWI directions were acquired: two directions perpendicular (⊥) and one parallel (∥) to the longitudinal spinal cord axis. The two perpendicular diffusion directions were averaged to increase the signal-to-noise ratio. The measurements were linearly regridded to be equidistant in q-space and the dPDF was computed using inverse Fast-Fourier-Transformation. To increase the resolution of the dPDF, the signal was extrapolated in q-space to a maximum q=166mm<sup>-1</sup> by fitting a bi-exponential decay curve to the DWI data<sup>4</sup>. From the dPDF we calculate the full width at maximum (FWHM) and zero displacement probability (P0) for each ROI in both ⊥ and ∥ directions.

**DTI protocol:** The DTI dataset contained 5 b=0 and 100 b=1000s/mm<sup>2</sup> DWI volumes with 20 gradient directions<sup>5</sup> repeated 5 times. The open-source Camino toolkit<sup>6</sup> was used to compute fractional anisotropy (FA), mean diffusivity (MD), axial diffusivity (AD) and radial diffusivity (RD) from the fitted tensor.

**ROI analysis:** We semi-automatically delineated the upper cervical spinal cord area between levels C2 and C3 on the b=0 images using an active surface segmentation<sup>3</sup> method separately for DTI and QSI. Each whole cord mask was then divided along the diagonal midlines into anterior (A), posterior (P), left (LL) and right (RL) lateral quadrants (see Figure 1 for illustration). The masks for each quadrant were eroded in-plane to ensure adequate separation between quadrants and minimise partial-volume contamination from CSF and grey matter. For both DTI and QSI datasets the average signal vector was computed for each quadrant before analysis as described above.

## RESULTS & DISCUSSION

Figure 2 shows two examples of computed dPDF curves for one healthy control and one patient. We observe much wider and more shallow dPDF ⊥ shapes in all quadrants in the patient, which indicates less hindered diffusion motion perpendicular to the long axis of the cord and can be associated with axonal damage and loss of fibre coherence over the whole cord<sup>7,8</sup>, perhaps in response to Wallerian degeneration distal to the site of injury. We find diffusion in the ipsilateral quadrant of injury most altered, which makes sense as the affected motor-neural projections pass mainly through this quadrant. Figure 3 shows DTI and QSI parameters in the ipsilateral and contralateral quadrants over all patients compared to healthy controls (LL and LR averaged in healthy controls). In the DTI data, FA is found to be lower and RD significantly increased in the ipsilateral quadrant of injury in patients compared to controls. In the QSI data, P0 ⊥ was equally decreased and FWHM ⊥ increased in the ipsilateral side, although the changes are more pronounced in QSI than in DTI. Furthermore, within the patients QSI appears more specific to the side of injury than DTI, showing statistically significant differences in both P0 ⊥ and FWHM ⊥ (p<0.01) between the ipsilateral and contralateral quadrants much stronger than in FA. Overall, the contralateral quadrant DTI and QSI changes are less apparent and not significantly different from healthy tissue (p>0.05 for all metrics vs healthy controls). Furthermore, none of the longitudinal diffusion characteristics (AD in DTI and P0 ∥/FWHM ∥ in QSI) show clear abnormalities in either quadrant.

**Correlations with clinical scores:** Significant correlations between clinical parameters and diffusion imaging markers are found in the posterior quadrant in VAS and DASH, but not MRC scores (see Figure 4 for the respective scatterplots). In patients, pain experienced as per VAS scores positively correlated with increase in P0 ∥ (Spearman's ρ =0.95, p<0.001) and also negatively with AD (ρ =-0.74, p<0.05). Furthermore, DASH disability scores correlated negatively with P0 ⊥ (ρ =-0.76, p<0.05). An increase in P0 ∥ indicates the presence of more diffusion barriers along the main white matter fibre direction. A decrease in P0 ⊥ means less presence of diffusion barriers perpendicular to the axonal fibres. In conjunction, these findings suggest an increase of isotropic restriction in the posterior quadrant. We speculate that this is explained by an increase in scar tissue or gliosis<sup>9</sup> resulting in more perceived pain and disability as reflected VAS and DASH scores.

## CONCLUSION

Our findings suggest that DTI and QSI of the upper cervical cord distal to the site of injury provide unique insights into the underlying pathological changes in BPA patients, suggesting the occurrence of axonal damage, and loss of fibre coherence, and potential gliosis. Furthermore we found that QSI provides diffusion imaging markers that correlate better with clinical markers of pain and disability than conventional DTI. Future work will increase the number of patients studied and will include also patients with BPA who did not undergo re-implantation, in order to further our understanding of the microstructure changes specific to re-implantation.

**REFERENCES:** 1. Carlstedt. *Microsurgery*. 1995 2. Callaghan. *J Phys E Sci Instrum*. 1988 3. Cook. *Proc of ISMRM*. 2006 4. Cook. *JMRI*. 2007 5. Farrell. *MRM*. 2008 6. Horsfield. *NeuroImage*. 2010 7. Beaulieu. *NMR in Biomed*. 2002 8. Ulug. *AJNR* 1999 9. Koliatsos. *J Comp Neuro*. 1994

We thank the MS Society of Great Britain and Northern Ireland, the ISRT and the Department of Health's NIHR Biomedical Research Centres funding scheme for support.

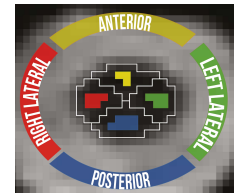


Figure 1: Color-coded quadrants overlaid on b=0 image.

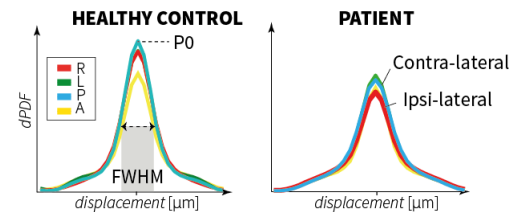


Figure 2: Computed dPDF ⊥ for the four quadrants in healthy control and patient

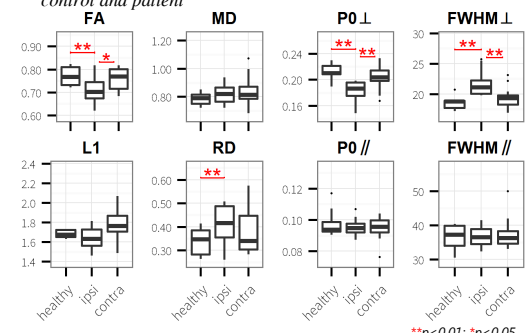


Figure 3: Boxplots of DTI (left) and QSI (right) metrics in lateral quadrants (healthy = LL and RL averaged in healthy controls, ipsi/contra=ipsi- and contralateral quadrant of BPA injury)

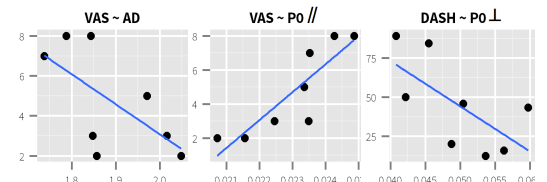


Figure 4: Scatterplots of clinical parameters (y-axis) and DWI metrics (x-axis) that show statistically significant correlations.